Available online at www.sciencedirect.com
ScienceDirect
Trans. Nonferrous Met. Soc. China 29(2019) 1705−1713
Transactions of Nonferrous Metals Society of China
www.tnmsc.cn

Microwave sintering of Mo nanopowder and its densification behavior

Bo-hua DUAN[1,2], Zhao ZHANG[1], De-zhi WANG[1,2], Tao ZHOU[1]

1. School of Materials Science and Engineering, Central South University, Changsha 410083, China;
2. Key Laboratory of Nonferrous Metal Materials Science and Engineering, Ministry of Education, Central South University, Changsha 410083, China

Received 12 December 2018; accepted 13 May 2019

Abstract: In order to prepare high-performance Mo with fine and homogeneous microstructure to meet the demand of high-technology applications such as metallurgical, mechanical, national defense, aerospace and electronics applications, the microwave sintering process and densification mechanism of Mo nanopowder were studied. In this experiment, Mo nanopowder and micropowder were used for conventional sintering and microwave sintering at different sintering temperatures and sintering time, respectively. The results showed that with the increase in the sintering temperature, the increase rates of the relative density and hardness increased rapidly at first and then slowed down. The relative density rapidly reached 95%, followed by a small change. Mo nanopowder with a relative density of 98.03% and average grain size of 3.6 μm was prepared by microwave sintering at 1873 K for 30 min. According to the analysis of the sintering kinetics, its densification is attributed to the combination of volumetric diffusion and grain boundary diffusion mechanisms. The calculated sintering activation energy of Mo nanopowder was 203.65 kJ/mol, which was considerably lower than that in the conventional sintering, suggesting that the microwave sintering was beneficial to the enhancement in the atom diffusion and densification for the powder. The results confirm that the microwave sintering is a promising method to economically prepare molybdenum with high properties.

Key words: molybdenum; microwave sintering; nanopowder; densification kinetics; diffusion mechanism

1 Introduction

As a refractory metal, molybdenum (Mo) is characterized by its high melting point (T_m=2893 K), high density (10.22 g/cm^3), high thermal conductivity and low coefficient of thermal expansion [1]. These properties make Mo appropriate for many high temperature applications such as nuclear energy materials, missile and aircraft parts, thermocouple sheaths, flame and corrosion resistant coatings for other metals [2−4]. Mo is often prepared by powder metallurgy method, where Mo micropowder is consolidated at a high temperature under a protective atmosphere (e.g., argon, nitrogen, and hydrogen); however, this method requires an extremely high sintering temperature, long sintering time and low heating rate, which leads to a coarse microstructure and deteriorates the mechanical properties. HUANG and HWANG [5] prepared Mo products with densities of 97% to 98.5% using a vacuum furnace at a sintering temperature of 2023 K with soaking time of 10 to 40 h.

In order to fabricate a Mo product having a fine and uniform microstructure, Mo nanopowder could be used as a raw material, owing to its high sintering activity. MAJUMDAR et al [6] reported the sintering of Mo nanopowder with average particle size of ~250 nm at a temperature of 2023 K for 60 min, yielding a sample with a relative density of 92%. However, the heating rate is still limited under the conventional heating mode, and short sintering time cannot meet the requirement of densification, while long sintering time inevitably leads to serious grain growth, low processability and deteriorated mechanical properties. Therefore, new sintering methods are recommended to achieve the rapid densification of the nanopowder. For example, spark plasma sintering (SPS) and microwave sintering are completely different from the conventional sintering [7−9]. Compared with the heating mechanism of radiation or conduction in the conventional sintering,

Foundation item: Project (2017YFB0305601) supported by the National Key R&D Program of China; Projects (51874368, 51274246) supported by the National Natural Science Foundation of China
Corresponding author: Bo-hua DUAN; Tel: +86-731-88877221; E-mail: duan-bh@csu.edu.cn
DOI: 10.1016/S1003-6326(19)65077-6

energy is directly transferred to the material by the coupling of electromagnetic waves, with the matter leading to volumetric heating in the microwave sintering [10−14]. This can accelerate the heating process and reduce both sintering temperature and sintering time, thus reducing the sintering time and saving energy. It also contributes to achieving the homogeneous and fine microstructure, and improving the mechanical properties. Microwave sintering was used for the first time in ceramic processing, and a series of materials such as Al_2O_3-doped alloys, W−Cu, Mo−Cu, WC−Co, W−Ni−Fe and metal matrix composites, were subsequently synthesized by this technology [15−20]. CHHILLAR et al [21] carried out microwave sintering of Mo micropowder for the first time. A high-density Mo product was obtained in a very short period of time, confirming the possibility of microwave sintering of pure Mo. However, there are still very few studies on the densification of Mo nanopowder under the microwave field. Therefore, the main objective of this study was to investigate the microwave sintering process of Mo nanopowder. Its densification kinetics was also discussed.

2 Experimental

2.1 Materials and methods

Mo nanopowder (average particle size: 40 nm, purity >99.95%, Shanghai Yaotian Co., Ltd., China) and Mo micropowder (average particle size: 40 μm, purity >99.9%, Beijing Daotian Co., Ltd., China) were used. The raw material Mo powder was dried in a vacuum drying oven (DZF, Beijing YGM Co., Ltd., China) at 333 K to prevent moisture and oxidation. The dried powder was then cold-pressed into a green compact with dimensions of *d*12 mm × 10 mm under different uniaxial pressures for 60 s. Finally, the green samples were placed into an HY−SZ4516 microwave sintering furnace (Hunan Huaye Co., Ltd., China) and sintered at a heating rate of 40 K/min to 1773, 1823 and 1873 K for 10, 20, 30 and 40 min, respectively. An infrared temperature measurement device was used to measure the temperature of the sample. In order to prevent the oxidation of Mo, the sintering process was carried out in vacuum and then the sample was cooled in 95% Ar + 5% H_2 atmosphere. A SiC slice was employed as a microwave susceptor to improve the overall heating effect.

For comparison, conventional sintering experiments were carried out on Mo nanopowder.

2.2 Characterization

The relative densities of the sintered samples were measured by the Archimedes principle. The microstructures and morphologies of the sintered samples were analyzed by environmental scanning electron microscopy (SEM, Quanta 200, FEI, Holland). Metallographic images of the sintered samples were observed by metallographic microscope (Leica CMIL LED, Germany). The contrast color of the metallographic image was adjusted for a better visualization of the grains and the color of the grain boundaries was set to be darker. The grain size was then measured by an image analysis software. The Vickers hardness of the sintered samples was tested by a Vickers microhardness meter (HVS−1000, Shanghai Luxin Co., Ltd., China) with a load of 0.3 kg for 15 s.

3 Results and discussion

3.1 Effect of green density on properties of microwave-sintered sample

The green density of the sample was controlled by adjusting the pressing pressure, and the results are shown in Fig. 1. With the increase in the pressure, the relative density initially rapidly increases to 66.05%. The increase rate starts to decrease at 300 MPa. The increased pressure is beneficial to the rearrangement of the powder with different particle sizes, thus expanding the contact area among the powders and increasing the green density. Moreover, a plastic deformation of the powder will occur when the pressing pressure is very high.

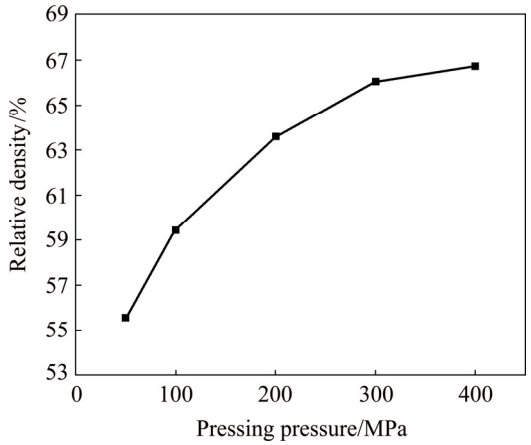

Fig. 1 Effect of pressing pressure on relative density of green sample

Figure 2 shows the effect of the green density on the relative density and hardness of the microwave-sintered samples. With the increase in the green density from 55.56% to 63.58%, the relative density of the sintered sample slowly increases from 96.8% to 98.0%, followed by the saturation. This is mainly attributed to the comprehensive effects of the following factors. The increase in green density expands the contact area among the powders, which improves the atom diffusion and densification of the powders during the sintering. On the

other hand, a higher green density leads to a higher reflection of the microwave energy, which reduces the coupling ability between the powder and microwave, thus impeding the densification of the powder. The results indicate that the green density has a small effect on the relative density of the microwave-sintered sample, and that the optimal green density should be controlled at 63%−67%.

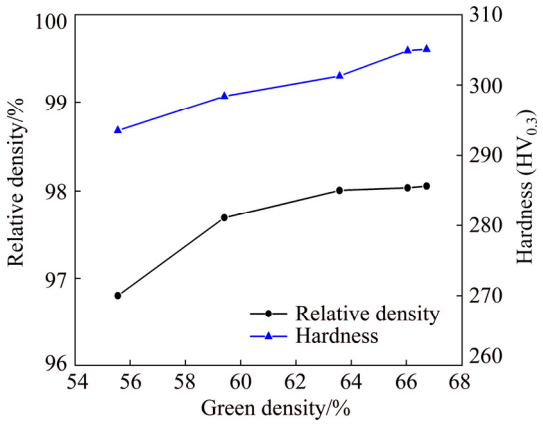

Fig. 2 Effect of green density on relative density and hardness of sintered samples

Figure 2 shows that the hardness of the sintered sample slowly increased with the green density. This can be attributed to the increased density of the sintered products and residual lattice distortion caused by the high pressing pressure.

3.2 Effect of sintering temperature on properties of sintered samples

Figure 3 presents the relative densities of the samples sintered at different temperatures for 30 min. Regardless of the sintering mode and powder size, with the increase in the sintering temperature, the relative densities of samples increase. This may be attributed to the enhancement in the atomic diffusion owing to the increased temperature. Compared with the Mo micropowder, the Mo nanopowder can effectively accelerate the densification process of the compact, yielding a higher density upon the microwave sintering. The skin depth (d) can be obtained as follows:

$$d = \frac{1}{\sqrt{\pi f \mu \sigma}} \tag{1}$$

where f is the microwave frequency, μ is the material magnetic permeability, and σ is the material electrical conductivity. According to Eq. (1), the skin depth of pure Mo at room temperature is approximately 8.61 μm. The conductivity of Mo decreases with the increase in the sintering temperature, while the skin depth of pure Mo increases (to approximately 23.19 μm at 1873 K). The particle size of the Mo nanopowder is considerably smaller than the skin depth, so the microwave energy can penetrate the powder to heat the compacts by volume heating. However, the particle size of the Mo micropowder is slightly larger than the skin depth. Therefore, the Mo micropowder cannot be completely heated; thus its density is considerably lower than that of the Mo nanopowder.

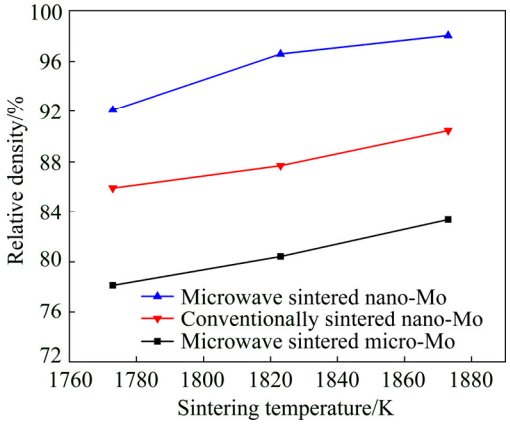

Fig. 3 Effects of sintering temperature on relative densities of samples

Figure 3 shows that the densities of samples after the microwave sintering are significantly higher than those of the conventional sintered samples under the same sintering conditions using the Mo nanopowder. During the microwave sintering, with the increase in the sintering temperature to 1823 K, the relative density initially rapidly increases to 96.57%. Subsequently, the densification rate of the Mo nanopowder considerably decreases, and the relative density reaches 98.03% after microwave sintering at 1873 K for 30 min, which is higher than that (~90.47%) obtained by the conventional sintering. This might be explained by the "non-thermal effects" of the alternating microwave electromagnetic field during the microwave sintering, which promote atomic diffusion [22,23].

Compared with the results of HUANG and HWANG [5], the relative density of the microwave-sintered Mo is similar; however, the sintering temperature and time in our experiment are considerably lower and shorter, respectively than the reported values (40 h at the temperature of 2173 K). This suggests that the microwave sintering can effectively increase the sintering density and reduce the sintering time, as it can reduce the sintering activation energy, and increase the diffusion driving force and diffusion rate. It has also been confirmed that the microwave sintering technique is advantageous for the rapid and high densification of pure Mo.

Figure 4 shows the effect of the sintering temperature on the hardness of samples. The change in hardness with the sintering temperature exhibits a similar

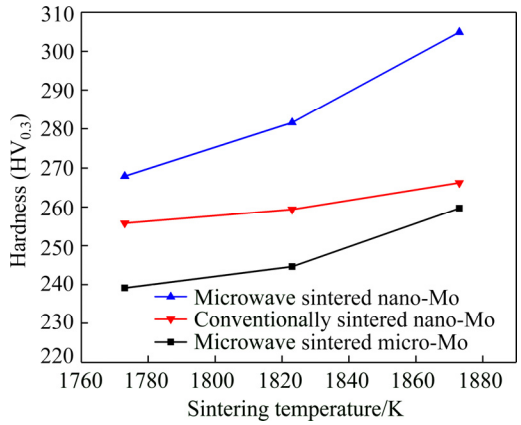

Fig. 4 Effect of sintering temperature on hardness of samples

trend to that of the relative density as the hardness of powder metallurgy product is determined mainly by its relative density and microstructure. The hardness is very sensitive to the porosity in the powder metallurgy process. With the decrease in the sintering density and the increase in the porosity, in the measurement of the hardness, the indenter simultaneously acts on the matrix and pores. The pores weaken the matrix and lead to the decrease in hardness. Generally, a higher density corresponds to a larger hardness.

Figure 5 reveals the optical microscopy (OM) images of the samples sintered at different temperatures. The microstructures of the microwave-sintered samples consist of uniform fine grains and well-dispersed pores. Figures 5(a−c) show the changes in the morphologies and sizes of the grains and pores. With the increase in the sintering temperature, the pores contract and their geometries tend to be circular. Figure 6 shows the grain size distribution of microwave-sintered samples. The average grain size slowly increases from 2.1 to 3.6 μm. With the increase in the microwave sintering temperature, the grain size of Mo slightly increases. The comparison of Figs. 5(c) and (d) shows that the microstructure of the microwave-sintered sample is more uniform, denser and finer than that of the conventionally sintered sample under the same sintering conditions, which is attributed to the lower sintering temperature, shorter sintering time, overall heating and unique "non-thermal effects" in the microwave sintering, leading to the improved mechanical properties and plastic deformation capacity of Mo. The grain size obtained in our experiment is even smaller than 7−9 μm reported by CHHILLAR et al [21].

Figure 7 exhibits SEM fracture micrographs of the microwave-sintered samples at different temperatures. The images present the typical brittleness fracture, which is similar to that of Mo prepared by the conventional process; some small pores and large number of sintered necks can also be observed. With the increase in the sintering temperature, the grain size slightly increases, while the size and number of pores significantly decrease and their shapes slowly evolve into circles from irregularities. In addition, the size of the sintered neck increases, which implies a remarkable improvement in the strength of the sintered sample.

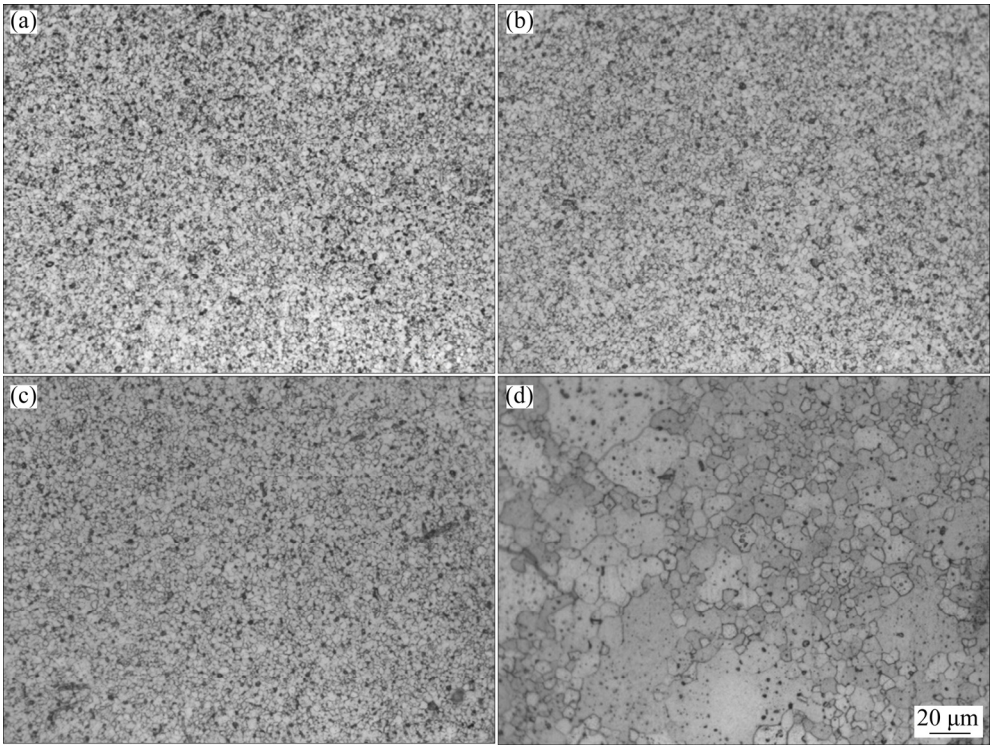

Fig. 5 OM images of samples obtained at different sintering temperatures of 1773 K (a), 1823 K (b), 1873 K(c), and conventionally sintered sample at 1873 K (d)

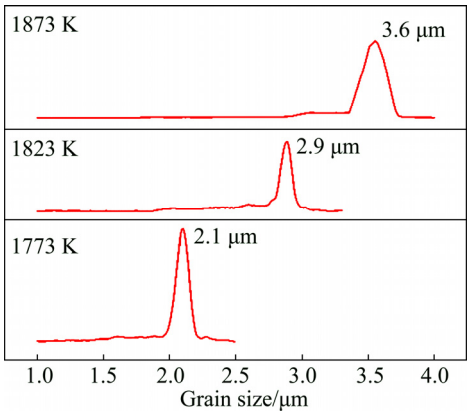

Fig. 6 Grain size distribution of samples microwave-sintered at different temperatures

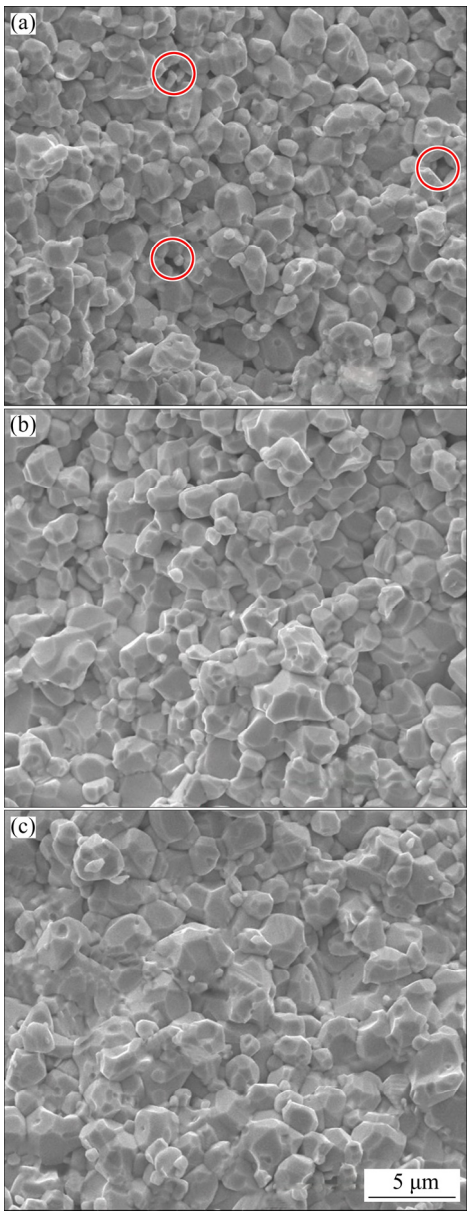

Fig. 7 SEM fracture micrographs of samples microwave-sintered at different temperatures: (a) 1773 K; (b) 1823 K; (c) 1873 K

3.3 Effect of sintering time on properties of sample

The relative density and hardness of the samples sintered at 1873 K and different time are shown in Fig. 8. The microwave sintering of samples sintered at 1873 K for 10 min rapidly provides a relative density and hardness of 95% and HV 297.9, respectively. With further increase in the sintering time, the relative density and hardness increase slowly. As shown in Fig. 9, the microstructures exhibit continuous small reductions in pore size and number accompanied with the small difference in grain size with the increase in the sintering time. The evolution of the microstructures is consistent with the results in Fig. 8. According to the conventional theory of powder metallurgy, the atomic diffusion rate is proportional to the square root of the sintering time. With the increase in the sintering time, sintering necks between powders form and grow, eventually leading to grain coarsening, while the size and number of pores initially rapidly decrease, and then the decrease rates become slow, followed by the transformation of the pore shape to spherical shape at the last sintering stage [24,25]. The experimental results seem to differ from the conventional theory. The microwave sintering can effectively reduce the activation energy of the atoms and considerably increase the atom migration rate and rearrangement opportunities, thus leading to the rapid densification of the Mo nanopowder within 10 min. Once the relative density of the sample is above 90%, it might significantly enhance the reflection of the microwave and shielding effect of the sample, which weakens the microwave coupling with the powder and prevents the grain growth and densification.

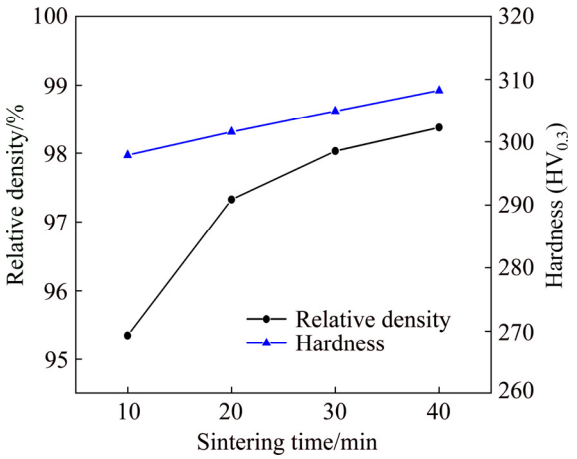

Fig. 8 Effect of sintering time on relative density and hardness of samples sintered at 1873 K

3.4 Microwave sintering kinetics

A sintering model can effectively quantify the sintering theory, and through the mathematical formula derivation, it is possible to determine the atom migration mechanism during the sintering.

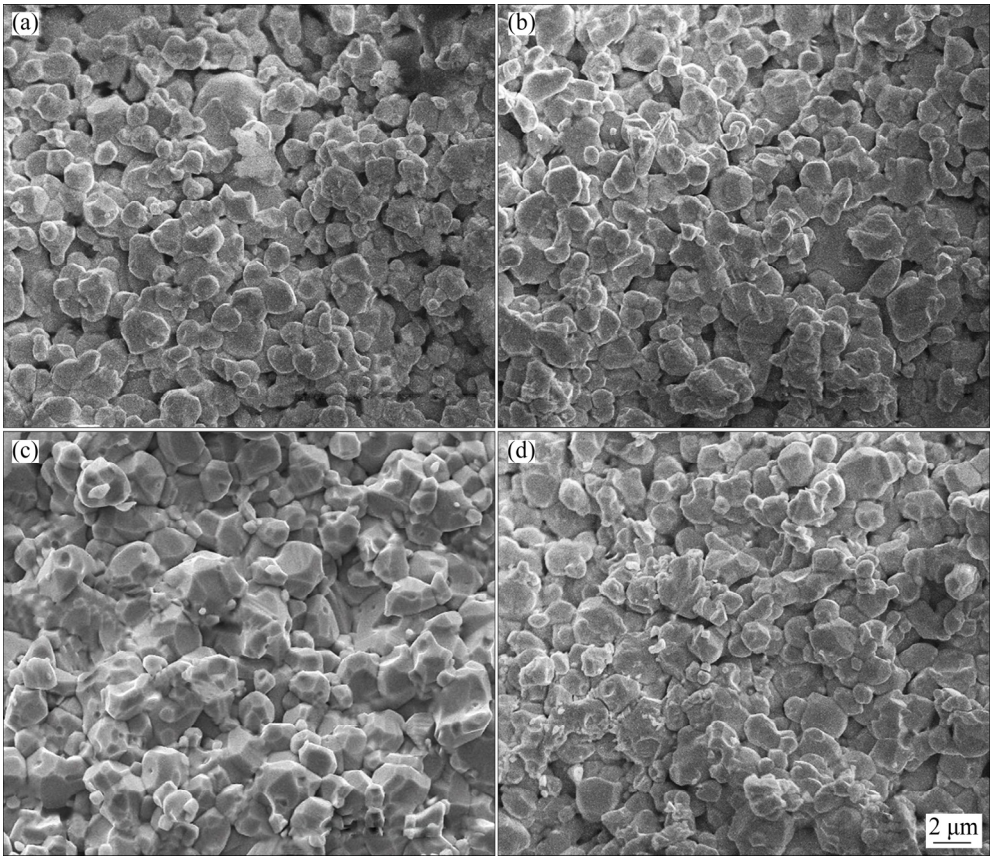

Fig. 9 SEM fracture micrographs of samples sintered for different sintering time: (a) 10 min; (b) 20 min; (c) 30 min; (d) 40 min

According to Eqs. (2) and (3) [26]:

$$\frac{\Delta L}{L_0} = A(T)t^{1/n} \tag{2}$$

$$\ln\frac{\Delta L}{L_0} = \ln A(T) + \frac{1}{n}\ln t \tag{3}$$

where $\Delta L/L_0$ is the relative shrinkage, $A(T)$ is a constant related to the sintering temperature, t is the sintering time, and n is the sintering characteristic index. The atom migration mechanism in the sintering process can be determined according to the value of n.

The relative shrinkage and transformation of the samples with different green densities sintered at 1773, 1823 and 1873 K for different sintering time are shown in Figs. 10 and 11, respectively. The shrinkage increases with the the increase of sintering time. By calculating the slope of the curve in Fig. 11, the sintering characteristic index n can be obtained, which is shown in Table 1.

The value of n slightly increases with the increase in the green relative density, but decreases with the increase in the sintering temperature. The kinetic characteristic index n reflects the main migration mechanism of the material in the sintering process. The volume diffusion is the main migration mechanism when n=2.5, while the grain boundary diffusion dominates in the process when n=3. If n is in the range of 2.5−3, the two mechanisms contribute during the sintering process. Therefore, the densification of the Mo nanopowder during the microwave sintering is attributed to the combination of the volumetric diffusion and grain boundary diffusion mechanisms. The value of n decreases with the increase in the sintering temperature, indicating that the tendency of volumetric diffusion increases. As the exchange speed between atoms and vacancies on the particle contact surface increases with the increase in the sintering temperature, the vacancies around the closed pores diffuse outside of the samples, thus enhancing the volumetric diffusion.

Table 1 Values of n in sintering kinetic equation

Green relative density/%	n		
	1773 K	1823 K	1873 K
60	2.857	2.741	2.609
63	2.884	2.760	2.622
66	2.896	2.768	2.627

By analyzing the activation energy, the material transport mechanism during the sintering process can be determined, which provides a theoretical basis for the development of a reasonable sintering process.

According to Eq. (4) [26]:

$$K=\frac{1}{t}=B\exp[-Q/(RT)] \tag{4}$$

where Q is the sintering activation energy, kJ/mol; T is the thermodynamic temperature，K; R is the molar gas constant, which is 8.314 J/(mol·K) and B is an experimental constant. After transformation of Fig. 4, we have

$$\ln t=\frac{Q}{RT}+\ln B' \tag{5}$$

where $\ln t$ linearly depends on $1/T$, Q/R is the slope of the line, and the sintering activation energy Q can be obtained according to the slope of the line.

By determining the value of $\ln(\Delta L/L_0)$ in Fig. 10, we can obtain three sets of values for $\ln t$ and $1/T$. Using $\ln t$ as the ordinate and $1/T$ as the abscissa, the relationship curves between these two parameters are presented in Fig. 12. By calculating the slopes of the lines, the activation energies Q under the microwave field for different green relative densities of 60%, 63% and 66% are calculated to be 208.14, 206.45 and 203.65 kJ/mol, respectively.

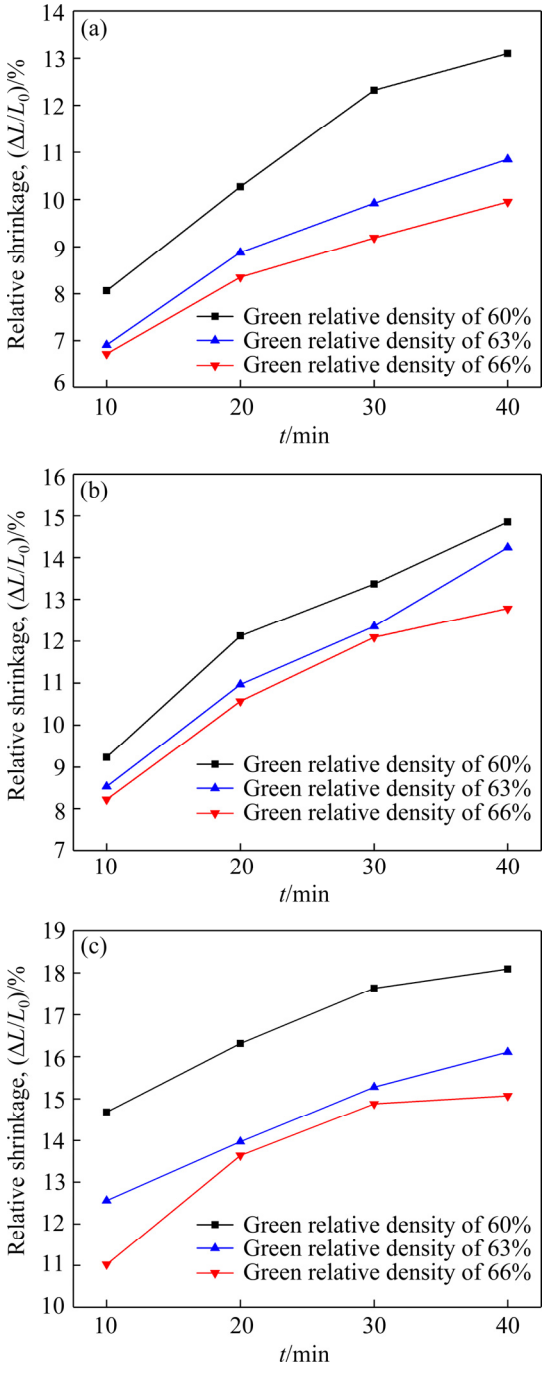

Fig. 10 Relative shrinkages of samples sintered at different temperatures: (a) 1773 K; (b) 1823 K; (c) 1873 K

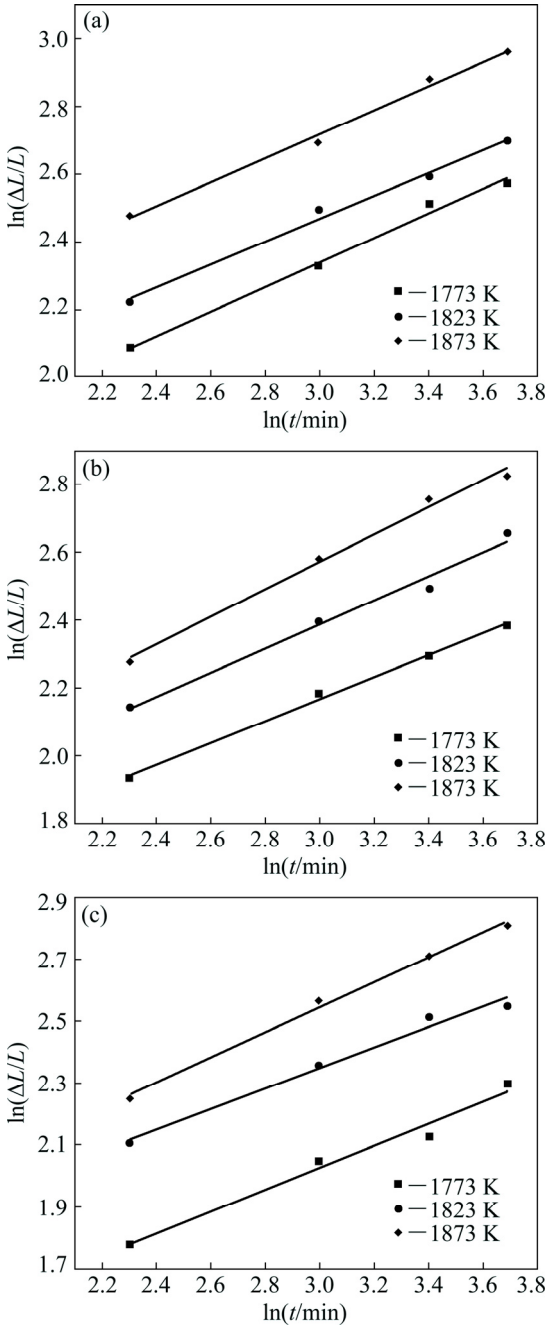

Fig. 11 Sintering kinetic curves of samples with different green relative densities and sintered at different temperatures: (a) 60%; (b) 63%; (c) 66 %

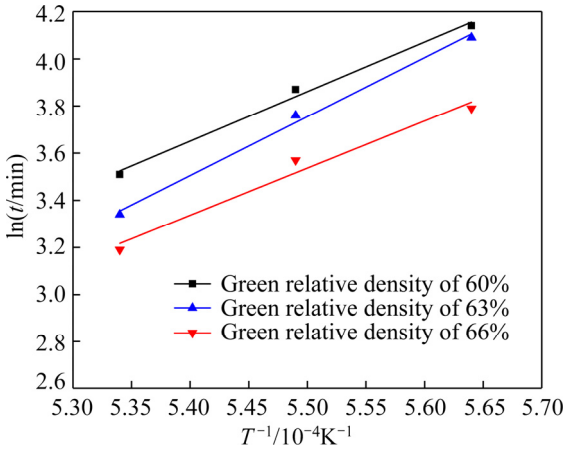

Fig. 12 Relationship curves between ln t and $1/T$

With the increase in the green density, the sintering activation energy slightly decreases. This may be attributed to the increase in the contact area and lattice distortion among the powders with the increase in the green density owing to the increased pressing pressure, which facilitates the atom diffusion. On the other hand, the trend of grain boundary diffusion slightly increases with the increase in the compact density at the same temperature, and the activation energy required for grain boundary diffusion is smaller than that of volumetric diffusion, so the sintering activation energy slightly decreases. Compared with the conventional sintering of pure Mo micro/submicropowder (Q is approximately 254 kJ/mol), the activation energy of the Mo nanopowder during the microwave sintering is effectively reduced. This is attributed to the high activity of the used nanopowder and assisted atom diffusion by the microwave field. Compared with the Mo micropowder, the Mo nanopowder has more grain boundaries and larger trend of grain boundary diffusion, leading to a lower sintering activation energy.

4 Conclusions

(1) With the increase in the microwave sintering temperature, the increase rates of the relative density and hardness of the Mo nanopowder initially increased and then decreased. The average grain size slowly increased from 2.1 to 3.6 μm, while the number and size of the pores decreased accompanied with their morphology change into spherical morphologies.

(2) The relative density rapidly reached 95% upon the microwave sintering for 10 min and subsequently slowly increased with the further increase in the sintering time, while the microstructure exhibited a small change. The Mo product with a relative density of 98.3%, and uniform and fine microstructure was rapidly prepared by the microwave sintering at 1873 K.

(3) The analysis of the sintering kinetics demonstrated that the densification of the Mo nanopowder during the microwave sintering was attributed to the combination of the volumetric diffusion and grain boundary diffusion mechanisms. Its sintering activation energy was only 203.65 kJ/mol, which is considerably lower than that in the conventional sintering, suggesting that the microwave field was beneficial to the enhancement in the atom diffusion and densification of the powder.

(4) Compared with the conventional sintering, the microwave sintering has advantages in terms of process time, cost, microstructure and properties of the sintered sample.

References

[1] LIU G, ZHANG G J, JIANG F, DING X D, SUN Y J, SUN J. Nanostructured high-strength molybdenum alloys with unprecedented tensile ductility [J]. Nature Materials, 2013, 12: 344−350.

[2] EL-GENK M S, TOURNIER J M. A review of refractory metal alloys and mechanically alloyed-oxide dispersion strengthened steels for space nuclear power systems [J]. Journal of Nuclear Materials, 2005, 340: 93−112.

[3] CHENG P M, ZHANG Z J, ZHANG G J, ZHANG J Y, WU K, LIU G, FU W, SUN J. Low cycle fatigue behaviors of pure Mo and Mo−La_2O_3 alloys [J]. Materials Science and Engineering A, 2017, 707: 295−305.

[4] WADSWORTH J, NIEH T G, STEPHENS J J. Recent advances in aerospace refractory metal alloys [J]. International Materials Reviews, 1988, 33: 131−150.

[5] HUANG H S, HWANG K S. Deoxidation of molybdenum during vacuum sintering [J]. Metallurgical and Materials Transactions A, 2002, 33: 657−664.

[6] MAJUMDAR S, RAVEENDRA S, SAMAJDAR I, BHARGAVA P, SHARMA I G. Densification and grain growth during isothermal sintering of Mo and mechanically alloyed Mo−TZM [J]. Acta Materialia, 2009, 57: 4158−4168.

[7] OHSER-WIEDEMANN R, MARTIN U, SEIFERT H J, MÜLLER A. Densification behaviour of pure molybdenum powder by spark plasma sintering [J]. International Journal of Refractory Metal and Hard Materials, 2010, 28: 550−557.

[8] MONDAL A, AGRAWAL D, UPADHYAYA A. Microwave sintering of refractory metals/alloys: W, Mo, Re, W−Cu, W−Ni−Cu and W−Ni−Fe alloys [J]. Journal of Microwave Power and Electromagnetic Energy, 2010, 44: 28−44.

[9] XIAO S L, TIAN J, XU L J, CHEN Y Y, YU H B, HAN J C. Microstructures and mechanical properties of TiAl alloy prepared by spark plasma sintering [J]. Transactions of Nonferrous Metals Society of China, 2009, 19: 1423−1427.

[10] DUAN B H, ZHOU Y, WANG D Z, ZHAO Y. Effect of CNTs content on the microstructures and properties of CNTs/Cu composite by microwave sintering [J]. Journal of Alloys Compound, 2019, 771: 498−504.

[11] MONDAL A, UPADHYAYA A, AGRAWAL D. Effect of heating mode on sintering of tungsten [J]. International Journal of Refractory Metal and Hard Materials, 2010, 28: 597−600.

[12] BAO R, YI J H, PENG Y D, ZHANG H Z. Effect of microwave sintering temperature and soaking time on microstructure of

WC−8Co [J]. Transactions of Nonferrous Metals Society of China, 2013, 23: 372−376.
[13] ZHANG N B, BAI C J, MA M Y, LI Z Y. Preparation of $BaAl_2O_4$ by microwave sintering [J]. Transactions of Nonferrous Metals Society of China, 2010, 20: 2020−2025.
[14] BAO R, YI J H, PENG Y D. Decarburization and improvement of ultra fine straight WC−8Co sintered via microwave sintering [J]. Transactions of Nonferrous Metals Society of China, 2012, 22: 853−857.
[15] XU L, YAN M, PENG J, SRINIVASAKANNAN C, XIA Y, ZHANG L. Influences of temperatures on tungsten copper alloy prepared by microwave sintering [J]. Journal of Alloys Compound, 2014, 611: 34−37.
[16] PRABHU G, CHAKRABORTY A, SARMA B. Microwave sintering of tungsten [J]. International Journal of Refractory Metal and Hard Materials, 2009, 27: 545−548.
[17] BAO R, YI J. Densification and alloying of microwave sintering WC−8wt.%Co composites [J]. International Journal of Refractory Metal and Hard Materials, 2014, 43: 269−275.
[18] YIN Z, YUAN J, CHENG Y, ZHANG Y, WANG Z, HU X. Microstructure evolution and densification kinetics of Al_2O_3/Ti(C,N) ceramic tool material by microwave sintering [J]. International Journal of Refractory Metal and Hard Materials, 2016, 61: 225−229.
[19] YANG B, SUN J, LI W, PENG J H, LI Y L, LOU H L, GUO S H. Numerical modeling dynamic process of multi-feed microwave heating of industrial solution media [J]. Transactions of Nonferrous Metals Society of China, 2016, 26: 3192−3203.
[20] DUAN B H, FU Z, QI C K, LIU H J, SUN A K, WANG D Z. Preparation of highly dispersed superfine W−20wt.%Cu composite powder with excellent sintering property by highly concentrated wet ball-milled process [J]. Rare Metals, 2018, 37: 961−967.
[21] CHHILLAR P, AGRAWAL D, ADAIR J H. Sintering of molybdenum metal powder using microwave energy [J]. Powder Metallurgy, 2008, 51: 182−187.
[22] ZUO F, SAUNIER S, MEUNIER C, GOEURIOT D. Non-thermal effect on densification kinetics during microwave sintering of α-alumina [J]. Scripta Materialia, 2013, 69: 331−333.
[23] SHAZMAN A, MIZRAHI S, COGAN U, SHIMONI E. Examining for possible non-thermal effects during heating in a microwave oven [J]. Food Chemistry, 2007, 103: 444−453.
[24] DEMIRSKYI D, AGRAWAL D, RAGULYA A. Neck growth kinetics during microwave sintering of nickel powder [J]. Journal of Alloys Compound, 2011, 509: 1790−1795.
[25] RAHIMIAN M, EHSANI N, PARVIN N, BAHARVANDI H. The effect of particle size, sintering temperature and sintering time on the properties of Al−Al_2O_3 composites, made by powder metallurgy [J]. Journal of Materials Process Technology, 2009, 209: 5387−5393.
[26] PÉREZ-MAQUEDA L A, CRIADO J M, REAL C. Kinetics of the initial stage of sintering from shrinkage data: Simultaneous determination of activation energy and kinetic model from a single non-isothermal experiment [J]. Journal of the American Ceramic Society, 2002, 85: 763−768.

纳米钼粉的微波烧结及致密化行为

段柏华[1,2]，张 钊[1]，王德志[1,2]，周 涛[1]

1. 中南大学 材料科学与工程学院，长沙 410083；
2. 中南大学 有色金属材料科学与工程教育部重点实验室，长沙 410083

摘 要：为了满足冶金、机械、国防、航空航天等高技术领域应用对组织均匀细小的高性能钼粉的需要，对纳米钼粉的微波烧结工艺和致密化机理进行研究。在本实验中，纳米钼粉和微米钼粉分别在不同温度和不同时间下进行常规烧结和微波烧结。结果表明：随着烧结温度的升高，相对密度和硬度的增速先快速增加随后增速减缓，相对密度迅速达到 95%，随后趋于稳定。采用微波烧结技术，在 1873 K 下烧结 30 min 获得相对密度为 98.03%、平均晶粒尺寸为 3.6 μm 的纳米钼粉。对纳米钼粉的微波烧结动力学进行研究，发现其致密化是体积扩散机制和晶界扩散机制共同作用的结果。计算得到的纳米钼粉的微波烧结激活能为 203.65 kJ/mol，远低于常规烧结方式的激活能，证明微波烧结有利于增强粉末的原子扩散性能和致密化过程。结果表明，微波烧结是制备高性能钼产品的一种经济可行的方法。

关键词：钼；微波烧结；纳米粉末；致密化动力学；扩散机制

(Edited by Wei-ping CHEN)